Experimental investigation on ion separation using a ceramic Nanofiltration membrane: influence of trans-membrane pressure and solution concentration on ion rejection

Rasha A. Hajarat*

hajarat@mutah.edu.jo

Abstract

The current research intends to conduct an experimental work to study the removal efficiency of Magnesium (Mg^{2+}), Potassium (K^{1+}), Sodium (Na^{1+}), Bromide (Br^{1-}) and Chloride (Cl^{1-}) ions from different prepared solutions using a ceramic Nanofiltration (NF) membrane with a molecular weight cut-off of 1 kDa. Specifically, the solutions are prepared using double ions and triple ions and the filtration is conducted using different operating conditions of the trans-membrane pressure (TMP) and ions concentrations. In this regard, the TMP ranges between 1 to 5 bar and the ion concentration ranged between 0.01 to 1.0 M (equivalent to 1.0 to 1000 mol/m^3). The results demonstrate that the highest ion rejection can be attained with the maximum applied TMP. However, this is not the case for the NaBr and KBr solutions, demonstrating the reverse action. Variable ion rejection patterns are experimentally identified in the current research, which varies between 90% to 99.7%.

Keyword: Nanofiltration membrane, NF, Rejection, Mg^{2+}, K^{1+}, Cl^{1-}, Na^{1+}, Br^{1-}, pore radius.

* Chemical Engineering Department, Engineering College, Mutah University, Jordan.

Received: 29/4/2025 . Accepted: 24/9 /2025 .

دراسة تجريبية لفصل الأيونات باستخدام غشاء ترشيح نانوي سيراميكي: تأثير الضغط عبر الغشاء وتركيز المحلول على رفض الأيونات

رشا الحجرات*

hajarat@mutah.edu.jo

ملخص

يهدف البحث الحالي إلى إجراء عمل تجريبي لدراسة كفاءة إزالة أيونات المغنيسيوم (Mg^{2+}) والبوتاسيوم (K^{1+}) والصوديوم (Na^{1+}) والبروميد (Br^{1+}) والكلوريد (Cl^{1-}) من محاليل مُحضرة مختلفة باستخدام غشاء ترشيح نانوي سيراميكية مع حد وزن جزيئي يبلغ 1 كيلو دالتون. على وجه التحديد، يتم تحضير المحاليل باستخدام أيونات مزدوجة وأيونات ثلاثية ويتم إجراء الترشيح باستخدام ظروف تشغيل مختلفة لضغط الغشاء (TMP) وتركيزات الأيونات. في هذا الصدد، يتراوح ضغط الغشاء (TMP) بين 1 إلى 5 بار ويتراوح تركيز الأيونات بين 0.01 إلى 1.0 مول (أي ما يعادل 1.0 إلى 1000 مول/م3). تُظهر النتائج أنه يمكن تحقيق أعلى رفض للأيونات باستخدام أقصى ضغط غشاء (TMP) مطبق. ومع ذلك، ليس هذا هو الوضع بالنسبة لمحاليل NaBr وKBr، والتي أظهرت التأثير العكسي. تم التعرف تجريبيا في البحث الحالي على أنماط رفض الأيونات المتغيرة، والتي تتراوح بين 90٪ إلى 99.7٪.

الكلمات المفتاحية: غشاء نانوي، رفض الغشاء، مغنيسيوم، بوتاسيوم، كلوريد، صوديوم، بروميد، نصف قطر المسام.

* قسم الهندسة الكيميائية، كلية الهندسة، جامعة مؤتة، الأردن.

تاريخ تقديم البحث: 2025/4/29م. تاريخ قبول البحث: 2025/9/24م.

Introduction

Nanofiltration (NF) membranes occupy a critical position between reverse osmosis and ultrafiltration technologies, offering selective separation capabilities for divalent ions and organic molecules. Though they exhibit fundamentally different characteristics, ceramic and polymeric membranes have emerged as prominent solutions across water treatment applications. Ceramic NF membranes leverage inorganic materials like alumina (Al_2O_3), zirconia (ZrO_2), and titania (TiO_2), providing exceptional chemical and thermal stability. In contrast, polymeric NF membranes predominantly utilize polyamide composites or polysulfone derivatives, offering advantages in manufacturing flexibility and initial cost efficiency (Mohanadas et al., 2022). Ceramic membranes feature asymmetric multi-layered structures with active layers of metal oxides (TiO_2, ZrO_2) on microporous supports. Ceramic NF characteristics (Table-1) include

a. Mechanical robustness: withstand pressures >20 bar and temperatures >100°C.
b. Chemical resistance: stable across pH 0-14 and resistant to oxidants (ozone, chlorine).
c. Surface charge properties: isoelectric points (IEP) of 6.1–9.5, enabling positive charge at low pH.
d. Pore size uniformity: MWCO range of 200-1,000 Da with narrow pore distributions.

Industrial implementations show long service lifetimes (>10 years) but face challenges with high manufacturing costs (2-5× polymeric equivalents) and limited module configurations. While in case of polymeric membranes dominate the market due to:

a. Lower production costs and modular design flexibility.
b. Higher initial permeability: typically, 10-30 liters per square meter per hour per bar (LMH/bar) vs. 1-10 LMH/bar for ceramics.
c. To create a tough and selective surface chemistry for specific applications: coatings such as zwitterionic or charged polymers can be significantly enhance surface selectivity.
d. pH limitations: polyamide layers degrade at pH < 2 or >11.
e. Oxidant susceptibility: chlorine/ozone exposure causes hydrolysis of amide bonds.

Property	Ceramic NF Membranes	Polymeric NF Membranes
Material Composition	Al_2O_3, TiO_2, ZrO_2	Polyamide, Polysulfone
pH Stability	0-14	3-11
Max Temperature	>100°C	<45°C
Oxidant Resistance	High (O_3, Cl_2 tolerant)	Low (Oxidant-sensitive)
Mechanical Strength	High (Compression-resistant)	Moderate (Prone to compaction)
Relative Cost	High ($500-1000/$m^2$)	Low ($50-200/$m^2$)
Lifespan	10-15 years	3-7 years

Table 1. Fundamental Properties Comparison between ceramic and polymeric NF.

Ceramic NF membranes demonstrate superior operational resilience in extreme chemical/thermal environments (e.g., oil production, acid mining), justifying their higher capital costs through extended service life and reduced cleaning requirements. Their positive charge characteristics enable unique applications in cation-dominated separations like lithium recovery (Kim et al., 2025). However, polymeric NF membranes retain significant advantages in applications requiring high anion rejection, pharmaceutical removal, or cost-sensitive deployments. Recent advances in fouling mitigation and acid-stable polymers continue to expand their operational envelope. The selection guidelines include:

- Choosing ceramic NF are preferable when: processing high-TSS streams, operating at pH<3 or >11, recovering high-value metals, or using ozone/chlorine cleaning
- Polymeric NF membranes are preferred for low-TOC waters, anion-dominated separations, budget-constrained projects, and when pharmaceutical removal is critical.

Future membrane development should prioritize ceramic membrane cost reduction and polymeric membrane durability enhancement to address current limitations. The convergence of both technologies through hybrid designs offers promising pathways toward next-generation NF systems with expanded capabilities. NF membrane has several applications in industries such as high-purity water production such as

- Polymerics dominate integrated membrane systems (MF/UF+RO+NF) for potable reuse, achieving 99.99% pathogen removal.
- Ceramic membranes show promise in ozone-integrated systems for direct NF of secondary effluent, but PPCP removal remains inadequate (<40%).

In addition, NF is used in resource recovery applications such as lithium extraction (Kirk et al., 2024). Where ceramic NF achieves 60-85% Li^{1+}/Na^{1+} selectivity in brine concentrates, leveraging positive charge at low pH values. Also, ceramic membranes maintain stability in acid mine drainage (pH<2) but show lower metal rejection than acid-resistant polymer NF membranes.

In addition, NF membrane is used in industrial wastewater treatment such as oilfield wastewater treatment (Cabrera et al., 2022). **Ceramic nanofiltration units operate for over 12,500 hours without any pretreatment, achieving 100% rejection of total suspended solids (TSS) and 85% ion rejection at an operating pressure of 16 bar.** While polymeric NF achieves >99% oil rejection from oily emulsions but it requires frequent cleaning (Mohanadas et al., 2022).

Nanofiltration (NF) membrane is classified as a pressure-driven membrane that falls between ultrafiltration and reverse osmosis membranes in terms of properties. While the permeate flux of NF membrane is greater than that of a reverse osmosis membrane, it offers a lower rejection rate (Kuusik et al., 2014). The separation process of a NF membrane involves various factors such as steric (sieving), electrostatic (Donnan) effects, convection, and diffusion (Schaefer et al., 2004). Specifically, this type of membrane shows low rejection for mono-valent ions and non-ionised organics weighing less than 150 g/mol, but high rejection for multi-valent ions and organics weighing more than 300 g/mol (Zhang et al., 2022). Ceramic NF membrane has a pore diameter ranging from 0.2 to 2 nm. Typically, these membranes are either positively or negatively charged form. One of the key benefits of NF membranes is their ability to operate at lower pressure in a comparison with reverse osmosis membranes (Alsarayreh et al., 2020), along with offering

selective rejection between mono-valent and multi-valent ions, and high permeate flux.

Fouling is a major drawback of NF membranes, resulting from foulants being adsorbed on pore walls, leading to pore blockage and surface fouling like cake and gel layer build-up (Jiang at al., 2017; Al-Obaidi et al., 2022). Specifically, two well-known types of NF membranes in the market include the polymeric and ceramic membranes. The current research emphasizes ceramic membranes. This membrane offers a reliable and flexible option for filtration and separation requirements. It has specific features that make it appropriate for various industries and applications (Arat, 2023).

The current research aims to evaluate the effectiveness of ceramic NF membrane for the removal of Mg^{2+}, K^{1+}, Na^{1+}, Br^{1-} and Cl^{1-} ions from various synthesised solutions. The solutions under consideration are $MgCl_2$, $MgBr_2$, and NaBr salts. In this aspect, it should be noted that the utilised methodology of this research has characterized by investigating the ions removal from both single salt solutions ($MgCl_2$, $MgBr_2$, and NaBr salts) or mixed salt solutions ($MgCl_2$ and KCl). The concentrations of these salts are varied between 0.1 and 1.0 mol/l.

Theory:

The concept of ions transport via the texture of the NF membrane is categorized by several different factors. These include the pressure difference across the membrane, concentration gradient, and electrical potential gradient. These are illustrated in the context of the extended Nernst-Planck equation (Schaefer et al., 2004)

$$j_i = K_{i,c} c_i J_v - D_{i,p} \frac{dc_i}{dx} - \frac{z_i c_i D_{i,p}}{RT} F \frac{d\Psi}{dx} \qquad (1)$$

where c_i is the concentration in the membrane (mol/m^3), $D_{i,p}$ is the hindered diffusivity (m^2/s), F is Faraday constant (C/mol), J_v is the volume flux based on the membrane area (m^3/m^2/s), j_i is the flux of ion (i) based on the membrane area (mol/m^2.s), $K_{i,c}$ is the hindrance factor for convection inside the membrane, R is the gas constant (J/mol.K), T is the absolute temperature (K), z_i is the valence of ion (i), and Ψ is the electrical potential (V). The Nernst-Planck equation is utilised in the current research to predict the ion observed rejection in terms of concentration and potential gradients,

$$R = 1 - \frac{C_{i,p}}{C_{i,f}} \qquad (2)$$

where $c_{i,f}$ is the ion (i) concentration in the feed solution (mol/m^3), $c_{i,p}$ is the ion (i) concentration in the permeate solution (mol/m^3), and R is the ion observed rejection.

The trans-membrane pressure (TMP) is an important parameter that identifies the necessary force to drive permeates through the texture of the membrane. TMP can be expressed as the difference in pressure across the membrane surface. Regarding the water treatment, a low TMP can ensure clean water and a clean membrane, compared to a high TMP, which results in a fouled membrane (Mdemagh et al., 2018). The TMP parameter signifies the average pressure between the inlet and outlet parts of the membrane module as demonstrated as follows

$$TMP = \left(\frac{P_{in}+P_{out}}{2}\right) - P_{permeate} \qquad (3)$$

where TMP is the Trans membrane pressure (bar), P_{in} is the pressure at the membrane feed side (bar), P_{out} is the pressure at the membrane retentate side (bar), and $P_{permeate}$ is the pressure at the membrane permeate side (bar). The pressure at the permeate side ($P_{permeate}$) is presumed to be equivalent to the atmospheric pressure (1 atm) (Al-Obaidi et al., 2018).

Increasing turbulence significantly at the feed side, for example by cross-flow, can reduce concentration polarization. This phenomenon otherwise diminishes membrane efficiency and affects observed rejection, as described in Eq. 2. However, the real rejection is commonly greater than the observed rejection since the real rejection concerns the concentration at the membrane wall (c_W). The real rejection (R_O) is depicted below,

$$R_o = 1 - \frac{C_{i,p}}{C_{i,w}} \qquad (4)$$

where $c_{i,w}$ the concentration at the membrane wall (mol/m^3). For a porous membrane; the flux obtained by assuming that the osmotic pressure is equal to the atmospheric pressure as elucidated as follows

$$J_v = \frac{\Delta P}{\eta R_M} \qquad (5)$$

where J_v is the volume flux based on the membrane area (m^3/m^2/s), ΔP is the trans-membrane pressure difference (N/m^2), R_M is the clean membrane

resistance (1/m) and η is the dynamic solvent viscosity (N.s/m^2). Consequently, the osmotic pressure can be obtained for a solution by knowing the membrane resistance. To obtain the membrane resistance, distilled water is used. The solution volumetric flux is determined by dividing the volumetric flow rate by the membrane surface area as depicted in the following equation,

$$J_v = \frac{Q}{A} \qquad (6)$$

where A is the membrane surface area (m^2), J_v is the volume flux based on the membrane area (m^3/m^2/s), and Q is the volumetric flow rate (m^3/s).

Experimental procedure

The tubular NF membrane used in the experiments was obtained from Sterlitech. Both active and support layers were made of TiO_2. The membrane consisted of seven channels, each measuring 250 mm in length, with an outside diameter (OD) of 10 mm, with a membrane total surface area of 0.013 m^2. One of the key characteristics of this membrane is its molecular weight cut-off of 1 kDa. This resource effectively filters out molecules exceeding 1 kDa in molecular weight, making it suitable for size-based separation application. Referring to the provided data from the manufacturer (Table 2), the membrane charge has a positive sign. Also, the membrane can handle a maximum operating pressure of 10 bars, a pH range of 0-14, and a maximum temperature of 250 ℃. The wide pH tolerance range, would permit the membrane to endure different acidic and alkaline conditions. This makes it a useful option for different applications in the industry, including pharmaceuticals, biotechnology, and food processing. Moreover, the temperature tolerance of less than 250 ℃, enables the use of membrane in several applications of high-temperature conditions. Its capacity to endure such temperatures can assure its consistency and durability in difficult conditions. Last but not least, the membrane can endure an operating pressure of above 10 bars, which indicates its capacity to withstand moderate levels of pressure during filtration processes. This characteristic would ensure the usefulness of the membrane and its efficacy in a wide sector of industrial applications where pressure is a central parameter.

Membrane properties	
Channels	7 channels
Channel length	250 mm
Outside diameter	10 mm
Surface area	0.013 m²
Pore radius	0.8 nm
Maximum molecular weight	1 kDa
pH Range	0 - 14
Temperature tolerance	Less than 250°C

Table 2. Membrane physical properties.

To evaluate the separation competencies of the ceramic NF membrane, water samples encompassing various types of salt solutions were exposed to desalination. Two scenarios were experienced: one with a mixture of $MgCl_2$ and KCl salts, and the other with a single salt solution consisting of $MgCl_2$, KCl, NaBr, and $MgBr_2$ salts. The concentrations of the solutions were selected as 0.1 to 1.0 M (10 to 1000 mol/m^3). Before testing the salt solutions, the membrane's efficiency was examined using distilled water. The intention was to explore whether fouling existed and to analyse the membrane's capacity to eliminate ions. By contrasting the results of the pure water and salt solution tests, the performance of the membrane in ion removal and the presence of fouling were appraised. The ion concentration, solution pH and conductivity were tested using Bante 900 benchtop multi-parameter meter. Bante 900 benchtop is a high-precision multi-parameter meter that comprises measurement modes for pH, oxidation-reduction potential (ORP), ion concentration, conductivity, TDS, salinity, resistivity and dissolved oxygen. The pH was controlled using BI-620 industrial online pH Controller.

The bench scale membrane setup, illustrated in Figure 1, comprises several components. These elements consist of a high-pressure pump, a 5-liter glass receptacle, a tubular stainless steel membrane module, a pressure-relief valve, sturdy flexible tubing, a pH/ORP controller, a pH/Ion/Conductivity meter, a scale, and a timer. At the core of the arrangement lies the tubular ceramic NF

membrane (TiO_2) with seven internal channels. Pressure regulation on the membrane surface was managed using valves, resulting in transmembrane pressure (TMP) values ranging from 1 to 5 bar as a result of valves controlling pressure regulation on the membrane surface.

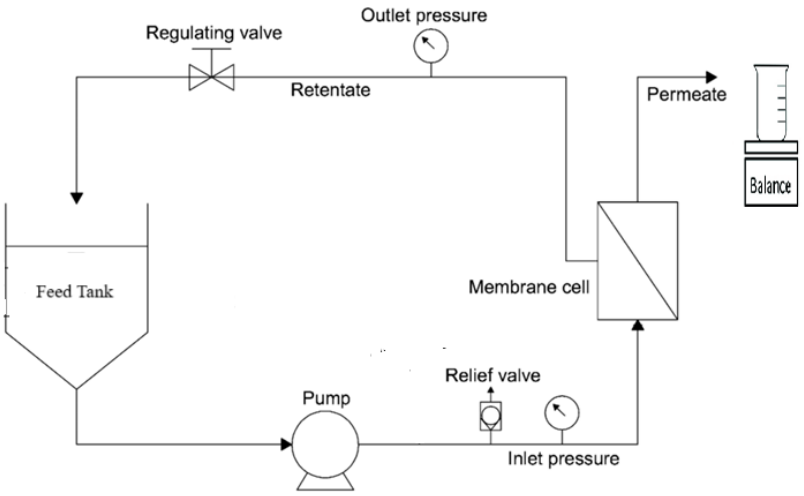

Figure 1. A schematic representation of the bench scale NF membrane set-up.

Results and discussion:

Different salts were used (single and double salts solutions) to compute the rejection of ions at different physical variables. The salts used in this study were KCl, NaBr, $MgBr_2$ and $MgCl_2$; thus, the studied ions would be Mg^{2+}, K^{1+} Na^{1+}, Br^{1}- and Cl^{1-} ions. The used concentrations for both cases, i.e., single and mixed salt solution; were 0.1, 0.5 and 1.0 mol/l. A ceramic NF membrane with a molecular weight cutoff of 1 kDa separated the ions at TMP ranging from 1 to 5 bar. **To ensure result consistency and assess separation accuracy, experiments for every salt and concentration combination were replicated a minimum of three times.**

Post-experiment membrane cleaning prevented fouling and restored baseline performance. The procedure involved: initial rinsing with distilled water until neutral pH was observed in permeate and retentate streams, followed by a one-hour cleaning cycle using 1.0 M NaOH solution, and finalized by thorough distilled water rinsing until neutral pH was re-established.

Magnesium chloride salt ($MgCl_2$) solution:

The used concentrations of magnesium chloride salt were 0.1, 0.5 and 1.0 M. It was noticed that the rejections of Mg^{2+} and Cl^{1-} increase as a response to increasing the TMP. The highest rejection was at TMP, which was equal to 5 bars. At the lowest concentration 0.1 M; the Mg^{2+} ion rejection at the lowest TMP was about 99%, while the Cl^{1-} ion rejection was about 96%. As the concentration of $MgCl_2$ increases, the rejection of Mg^{2+} and Cl^{1-} ions decreases (Figure 2). This would be as a response of concentration polarisation on the membrane surface triggering the ion to pass through the texture of the membrane. Concentration polarisation would cause Mg^{2+} and Cl^{1-} ions to cover the membrane surface and cause the membrane surface active charge to be neutralised. In such case; the rejection of Mg^{2+} and Cl^{1-} ions was increased due to increasing the TMP and decreasing the ions concentration in the solutions. Thus, the active membrane surface charge is neutralised, TMP would force Mg^{2+} and Cl^{1-} ions to diffuse through the membrane; as a result, the rejection of Mg^{2+} and Cl^{1-} ions is lowered (Dutta et al., 2020).

The Mg^{2+} ion rejection is greater than the Cl^{1-} ion rejection. This can be attributed to the positive charge of the Mg^{2+} ion. The membrane surface active layer charge is known to have a positive charge and in response to the repulsion between Mg^{2+} ions and the membrane charge, Mg^{2+} ions are rejected back to the feed solution where they leave the membrane on the retentate side.

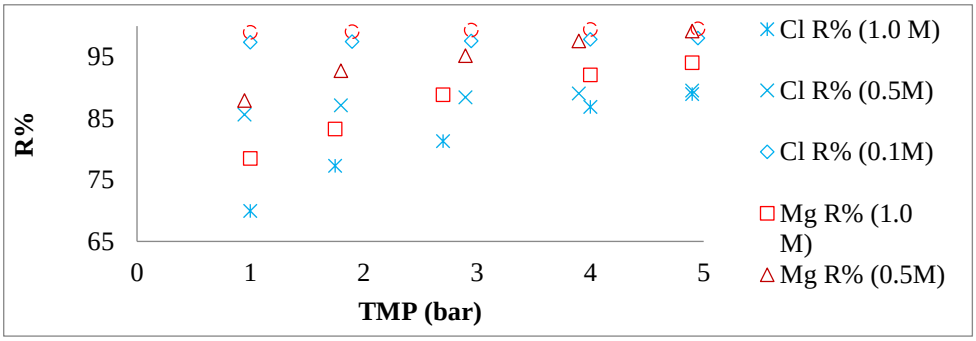

Figure 2. Rejection of Mg^{1+} ion and Cl^{1-} ion against TMP at different solution concentrations

After each run of $MgCl_2$; the membrane was cleaned and a distilled water experiment was run to ensure that fouling did not occur. For the distilled water experiment; the correlation between the flux and TMP was higher than that

for $MgCl_2$. The membrane did not return to its original virgin condition even after cleaning the membrane. Measurement of **distilled water flux** before/after cleaning vs. virgin may have different results which are

1. **Increased Rejection + Reduced Flux: indicates** a strong indicator of pore narrowing.
2. **Decreased Rejection + Increased Flux:** indicates damage or foulant removal exposing larger pores.
3. **Reduced Flux + Stable Rejection:** indicates surface coverage or pore blocking without significantly altering the smallest pores.

Thus, in this case, it was the third case that was supported by the obtained results. **In Summary of the ceramic NF** membrane, the failure to return to the virgin state is **NOT due to solvent swelling**. It is far more likely to be caused by

a) **Dissolution and re-deposition** forming a pore-narrowing gel layer ("covering").

b) **Irreversible adsorption/chemisorption** of foulants or cleaning agents onto the ceramic surface.

c) **Residues/precipitates** from cleaning agents are blocking pores.

d) **Microstructural damage** from overly aggressive cleaning (Less likely).

In fact, the membrane resistance (R_m) was measured using distilled water. The membrane resistance (R_m) was obtained using Eq. 5. Figure 3 shows the distilled water flux (J_v) versus TMP where the obtained slope was 1E-05. Applying both the obtained slope and water dynamic viscosity, which equals 1.002E-3 N.s/m^2 in Eq. 5, the membrane resistance (R_m) was found to be 9.98E+12 (1/m).

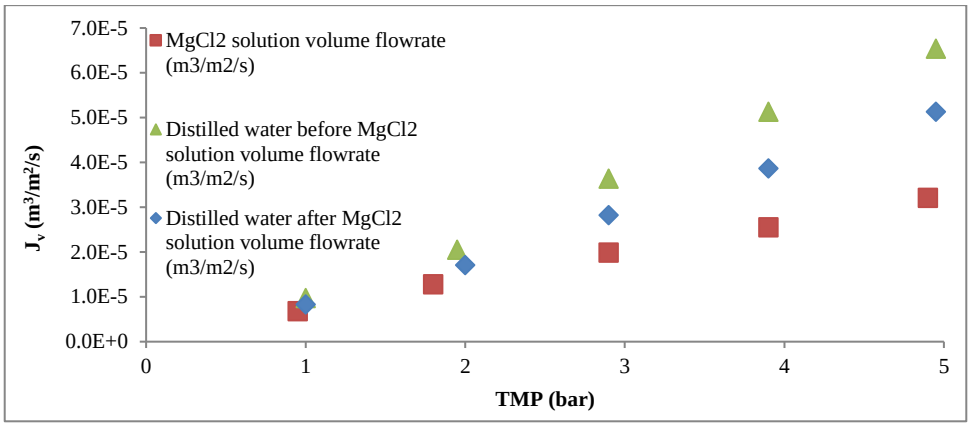

Figure 3. $MgCl_2$ solution and distilled water Flux against TMP

Magnesium bromide salt ($MgBr_2$) solution:

For the magnesium bromide salt case, the used concentrations are 0.01, 0.1 and 0.5 M. It was observed that the rejections of Mg^{2+} and Br^{1-} can be increased as the TMP increases. In this aspect, the greatest rejection was at TMP of 5 bars. For Mg^{2+} ions, the rejection upsurges with increasing concentration. Similarly, the same concept is valid for Br^{1-} ions, as the rejection increases, the concentration also increases. At the highest concentration of 0.5 M, the rejection of Mg^{2+} ion at maximum TMP was about 99.5%. However, the rejection of Br^{1-} was about 99.7%. These behaviours can be noticed in Figure 4.

The minimum rejection of 95.7% for Mg^{2+} ion was ascertained at a TMP of 1 bar and a concentration of 0.01 M. On the other hand, the minimum rejection of Br^{1-} was 98.2% at 1 bar TMP. These results are due to an ionic radius of 0.072 nm for Mg^{2+} and 0.195 nm for Br^{1-} (Shannon, 1967). The volume of Br^{1-} ions is larger than Mg^{2+} ions, and therefore the Br^{1-} would be rejected by the membrane and Mg^{2+} would diffuse through the membrane pores more easily.

The membrane surface and the ion charges impact the rejection of Mg^{2+} and Br^{1-} ions. Since the membrane surface charge is positive, Mg^{2+} ions are repelled, resulting in rejection. However, the attraction occurs between the Br^{1-} ions and the membrane charge, causing the Br^{1-} ions to deposit on the membrane surface and be rejected. Such conditions cause concentration polarisation, where Mg^{2+} and Br^{1-} ions cover the membrane surface and cause the membrane surface active charge to be neutralised. The polarisation

layer would cause the Mg^{2+} and Br^{1-} ions to be rejected. As a result, the decrease of Mg^{2+} and Br^{1-} ions rejection is because of ions diffusion through the membrane, where the membrane surface charge is neutralised (Zhang et al., 2022).

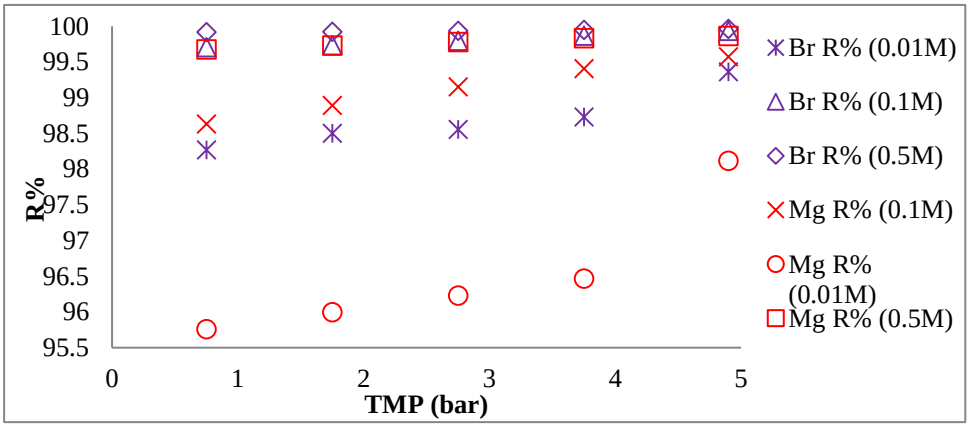

Figure 4. Rejection of Mg^{2+} and Br^{1-} ions against TMP at different solution concentrations (0.01, 0.1 and 0.5 M)

TMP	J_v (m^3/m^2 /s) x 10^{-6}	R% Mg (0.01 M)	R% Br (0.01 M)	R% Mg (0.1 M)	R% Br (0.1 M)	R% Mg (0.5 M)	R% Br (0.5 M)
0.75	5.34	95.76	98.27	98.63	99.71	99.68	99.92
1.75	8.97	95.99	98.50	98.89338189	99.74	99.68	99.92
2.75	0.141	96.23	98.56	99.15	99.80	99.68	99.92
3.75	0.218	96.46	98.73	99.41	99.87	99.68	99.92
4.9	0.256	98.11	99.37	99.58	99.94	99.68	99.92

Table 3. Rejection of Mg2+ and Br1- ions against TMP at different solution concentrations (0.01, 0.1 and 0.5 M)

The rejection behavior of $MgBr_2$ diverges significantly from $MgCl_2$ due to anion-specific effects arising from differences in hydrated size and charge interactions. While both salts contain Mg^{2+} cations (experiencing electrostatic repulsion from the positively charged membrane), replacing Cl^- with larger Br^- anions alter concentration polarization dynamics and charge neutralization rates, directly impacting Mg^{2+} rejection. Br^{1-} has a larger hydrated radius (0.196 nm) compared to Cl^{1-} (0.181 nm) (Shannon, 1976). Larger ion size reduces Br^{1-} diffusivity (Br^{1-}: 2.08×10^{-9} m²/s; Cl^{1-} : 2.03×10^{-9} m²/s), thus slowing its back-diffusion from the membrane surface. In the case of $MgBr_2$; Br^{1-}'s low diffusivity causes rapid accumulation at the membrane surface due to electrostatic attraction. This forms a denser concentration polarization layer enriched in both Br^- (attracted) and Mg^{2+} (repelled but trapped). Moreover, for the case of $MgCl_2$; Cl^{1-}'s higher mobility enables partial dissipation of the concentration polarization layer via back-diffusion, resulting in weaker polarization. In $MgBr_2$, the dense Br^{1-} rich concentration polarization layer more effectively shields/screens the positive membrane charge than Cl^{1-}. This accelerates neutralization of surface charge, diminishing electrostatic repulsion of Mg^{2+}.

The impact on Mg^{2+} ion rejection; in the case of $MgCl_2$ a moderate charge screening occurs; Mg^{2+} rejection remains high due to persistent repulsion. While in the case of $MgBr_2$; rapid charge neutralization weakens Mg^{2+} repulsion, enabling greater diffusion through the membrane and a significant drop in Mg^{2+} rejection. Despite electrostatic attraction with the membrane positive surface charge, both Cl^{1-} and Br^{1-} exhibit high rejection due to size exclusion; where larger hydrated Br^- is sterically hindered. Concentration polarization drives rejection accumulated anions which create a concentration gradient driving back-diffusion.

Sodium bromide salt (NaBr) solution:

The utilised concentrations of sodium bromide (NaBr) salt were 0.01, 0.1 and 0.5 M. It was revealed that the rejection of Na^{1+} and Br^{1-} ions decreases as the TMP increases. Figure 5 indicates that the rejection of Na^{1+} and Br^{1-} ions increases with increased feed concentrations. In this regard, the maximum rejection for Br^{1-} ions of 99.25% was at 0.1 M compared to 99.1% for Na^{1+} ions at 0.5 M (Figure 5). The rejection of Na^{1+} and Br^{1-} ions would result from the applied pressure on the membrane surface and the ions charge. A repulsion occurs between the positive membrane surface charge and the Na^{1+} ions. Referring to the charge repulsion, Na^{1+} ion would not pass through the membrane pores and would go back from the membrane surface area to

the feed bulk solution causing an increase in Na^{1+} ion rejection. However, the attraction occurred between the positive membrane surface charge and the negative charge of Br^{1-} ion. Consequently, the Br^{1-} ions would accumulate on the membrane surface. The accumulated Br^{1-} ions on the membrane pore surface would pass through the membrane pores to the permeate side causing the decrease of Br^{1-} ion as the TMP increases. These results were confirmed by Moslemi et al., (2012) where Br^{1-} ions can be separated from water using a ceramic NF membrane.

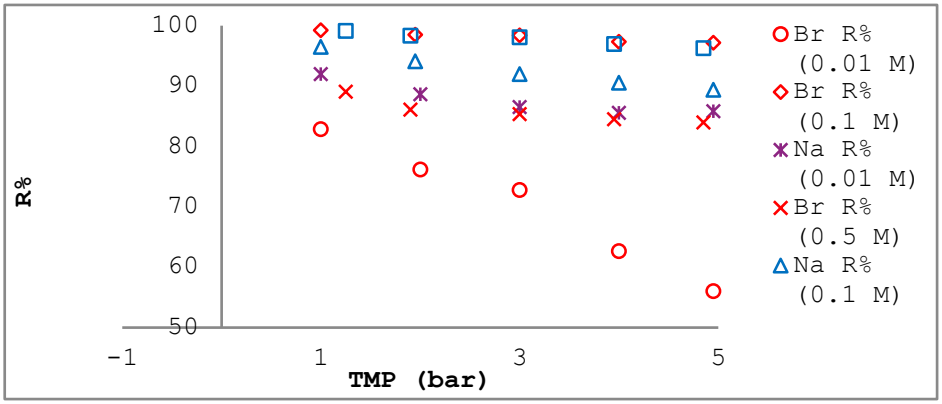

Figure 5. Rejection of Na^{1+} ion and Br^{1-} ions against TMP at different solution concentrations (0.01, 0.1 and 0.5 M)

Potassium chloride (KCl) and magnesium chloride ($MgCl_2$) solution:

The salts used to prepare the mixed salts solution are potassium chloride (KCl), and magnesium chloride ($MgCl_2$). The solution was prepared by mixing KCl and $MgCl_2$ to obtain three different solutions with the concentrations of 0.1, 0.5 and 1.0 M. Indeed, the obtained ions are Mg^{2+}, K^{1+} and Cl^{1-}. A decrease in the rejections of Mg^{1+}, K^{1+}, and Cl^{1-} was noticed as a response to decreasing the solution concentration and increasing the TMP. For instance, the highest rejection for Mg^{2+} was close to 90% at a TMP equal to 1 bar at a solution concentration of 1.0 M. The Mg^{2+} ion rejection decreased with the increase in TMP and the decrease in solution concentration. These results can be seen in figures 6 and 7. In the case of K^{1+} ions rejection, it decreased as TMP increased. In fact, its rejection was less than the rejections of Mg^{2+} and Cl^{1-} ions (Figure 6). However, when a solution concentration of 0.1 and 1.0 M was used, the rejection of K^{1+} ion was higher than the rejection of Mg^{2+} ions. Figures 8 and 10 can support this argument clearly.

Regarding Cl^{1-} ions, a decrease in rejection exists when there is an increase in TMP and a decrease in solution concentration. The greatest rejection of Cl^{1-} ion was at a TMP of 1 bar and a solution concentration of 1.0 M as demonstrated in Figure 6. This type of rejection is due to the charges of the ions and the membrane surface as the membrane selective layer is positively charged. Meanwhile, the membrane surface charge is positive, a repulsion between the membrane charge and Mg^{2+} and K^{1+} ions occur, reducing their rejection. Meanwhile, Mg^{2+} ions have a double ion charge but the K^{1+} ions have a single ion charge. The Mg^{2+} rejection was higher due to its larger repulsion force as depicted in Figure 6. The distilled water flux (J_v) and $MgCl_2$ and KCl solution flux (J_v) were measured. **Figure 7 shows the relationship between flux (J_v) and transmembrane pressure (TMP).** It can be assured that the distilled water line was above the $MgCl_2$ and KCl solution lines; hence fouling did not take place during the $MgCl_2$ and KCl solution experiments (but a polarization would have taken place). Thus, the concentration polarisation would support rejecting behaviour of Mg^{1+}, K^{1+}, and Cl^{1-} ions. At higher concentrations, a polarisation effect would increase causing a higher charge on the membrane surface causing an effect on the ion's rejection. This was obvious in the case of Mg^{2+} where its rejection was at its lowest when TMP increases as shown in Figures 6. This is already declared in the experimental results (Carvalho et al., 2011).

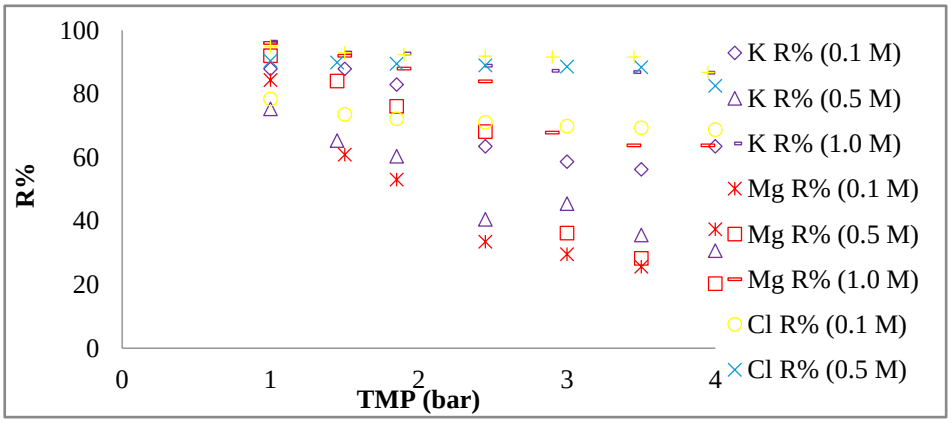

Figure 6. Rejection of Mg^{2+}, K^{1+} and Cl^{1-} ions against TMP for solution concentration of 0.1, 0.5 and 1.0 M.

Once the mixture of KCl and $MgCl_2$ was utilized in the separation process, membrane resistance (R_m) can be calculated by Eq. 6. From the plot of distilled water flux (J_v) versus TMP in Figure 7, a slope of 1E-5 to 6E-6 was determined. This slope yields a membrane resistance (R_m) of 1.33E+13 m^{-1}.

It is therefore concluded that the membrane resistance affected the ion's separation.

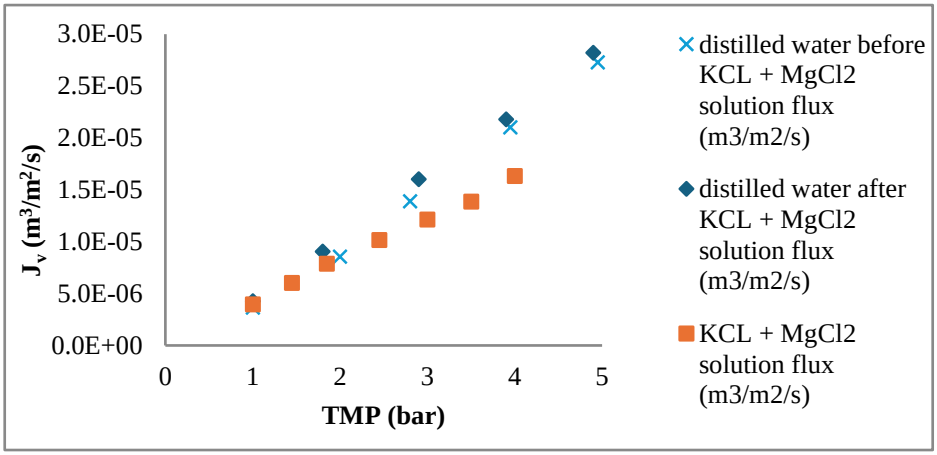

Figure 7. Volumetric flux (J_v) ($m^3/m^2/s$) versus TMP (bar)

The assessment of the flux of distilled water prior to and after the cleaning process may yield varied outcomes, which include:

An increase in rejection combined with a reduction in flux serves as a robust indicator of pore constriction. A decrease in rejection alongside an increase in flux; this suggests either damage or the removal of foulants, thereby revealing larger pores. A reduction in flux coupled with stable rejection; this signifies surface coverage or pore obstruction without substantially affecting the smallest pores.

Consequently, in this particular instance, the results substantiated the third scenario. In conclusion, the ceramic NF membrane's inability to revert to its virgin state is NOT attributable to solvent swelling. It is significantly more probable that this phenomenon is induced by:

The dissolution and subsequent re-deposition result in a gel layer that narrows the pores ("covering"). The irreversible adsorption or chemisorption of foulants or cleaning agents onto the ceramic surface. The presence of residues or precipitates from cleaning agents obstructing the pores. Microstructural damage resulting from excessively aggressive cleaning practices.

Sodium bromide (NaBr) and potassium bromide (KBr):

The utilised solutions were prepared for section by mixing sodium bromide (NaBr) and potassium bromide (KBr). The original solutions had three different concentrations of 0.1, 0.5 and 1.0 M and therefore the obtained ions are Na^{1+}, K^{1+} and Br^{1-}. Na^{1+}, K^{1+}, and Br^{1-} rejections decrease as the TMP increases. Figures 8-10 reveal the highest rejection for K^{1+} of around 99.8% at a TMP of 1 bar at a solution concentration of 1.0 M. Furthermore, the Na^{1+} ion has the highest rejection is 99% at a concentration of 0.1 M and a TMP of 1 bar. Lastly, the Br^{1-} ions highest rejection equals 99% at a TMP of 1 bar and a concentration of 0.1 M.

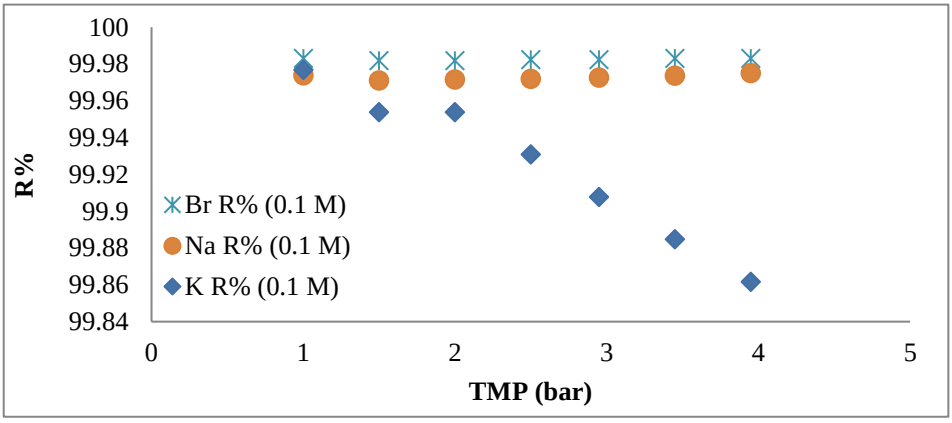

Figure 8. Rejection of Na^{1+}, K^{1+} and Br^{1-} ions against TMP at 0.1 M

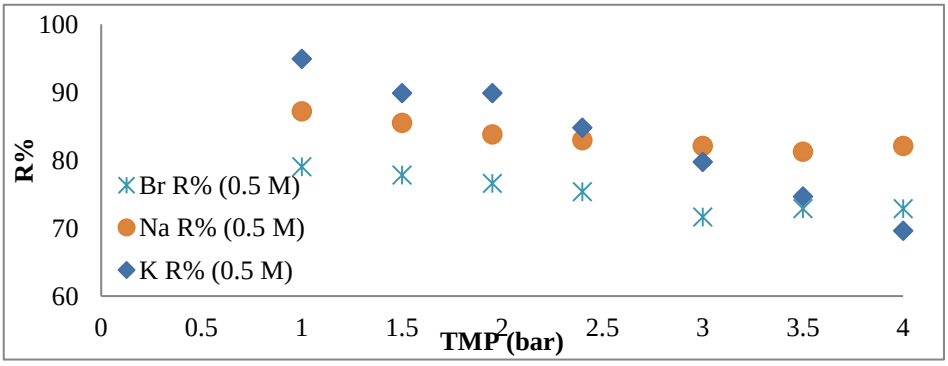

Figure 9. Rejection of Na^{1+}, K^{1+} and Br^{1-} ions against TMP at 0.5 M

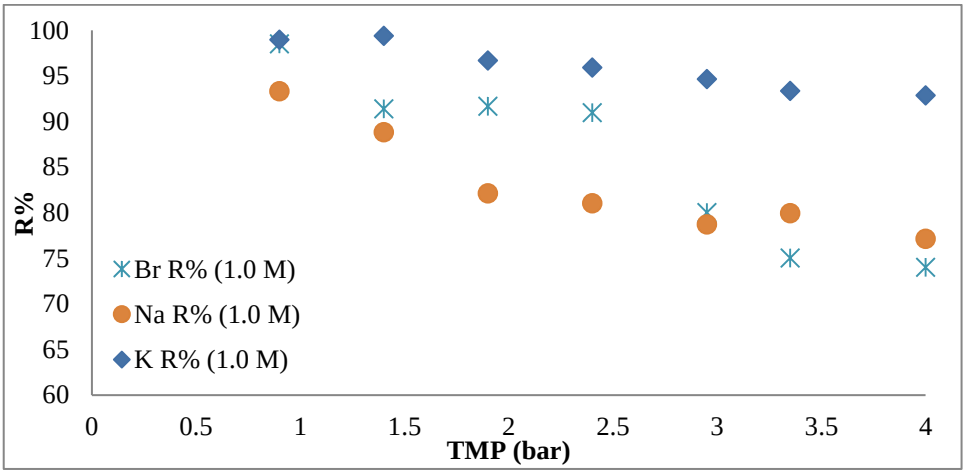

Figure 10. Rejection of Na^{1+}, K^{1+} and Br^{1-} ions against TMP at 1 M

Therefore, it can be said that the rejections of Na^{1+} and Br^{1-} ions are increased as the concentration decreases. The rejection of Na^{1+} ion was the lowest compared to the rejection of K^{1+} and Br^{1-} ions. The rejections of Na^{1+}, K^{1+}, and Br^{1-} would be due to the ions charge and membrane surface charge, where the membrane selective layer is positive. Since the membrane surface charge is positive, a repulsion between the membrane charge and Na^{1+} and K^{1+} exists thus increasing their rejection. The attraction between the membrane surface's selective charge and the Br^{1-} ions causes the ions not to be rejected.

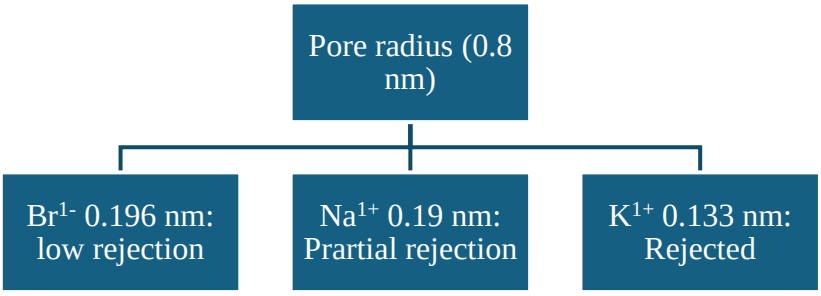

Figure 11. Pore size and ions diameter rejection behavior.

On the other hand, as the concentration of Na^{1+}, K^{1+} and Br^{1-} ions increases; then Na^{1+} and K^{1+} ions would neutralise the membrane surface charge causing the electrical potential to be negligible. Thus, at high ions concentration, the high rejection for the three ions Na^{1+}, K^{1+} and Br^{1-} ions would result from TMP as driving force. Here convection and diffusion potentials would overcome the electrical potential (Figure 11-13). Diffusion is the movement of individual molecules from a region of higher concentration to a region of lower concentration. Thus Na^{1+}, K^{1+} and Br^{1-} ions would from membrane's feed side (high concentration region) to the membrane's permeate side of the membrane (low concentration region). As the concentration decreases, the rejection of the Br^{1-} ions increases. Moreover, the rejection of Na^{1-} ions was greater than that of K^{1+} ions. As a result, the ion size would have a more significant effect on the ion rejection than the electrical potential force. As TMP increases; the applied pressure would force the ions to diffuse through the membrane causing ion rejection to decrease. It is acknowledged that the radius of K^{1+} ion is 0.133 nm, Na^{1+} ion is 0.19 nm, and Br^{1-} ion is 0.196 nm (Shannon, 1976). Thus, the diffusion potential due to the pressure difference across the membrane had more effect than the concentration gradient and the electrical potential gradient. It is important to consider all of the concentration gradient, the electrical potential gradient and the related ions concentration.

At elevated Na^{1+}, K^{1+}, and Br^{1-} ions concentrations, charge screening neutralizes the membrane surface charge, rendering the electrical potential negligible. Consequently, high rejection of these ions at high ionic strength is primarily driven by **transmembrane pressure (TMP)**. Under these conditions, **convective transport** (pressure-driven flow) and **diffusion** (ion movement down concentration gradients) dominate over diminished electrostatic forces (Figures 11-13).

Diffusion specifically describes net ion migration from high-concentration regions (feed) to low-concentration regions (permeate). As bulk ion concentration **decreases**, Br^{1-} rejection **increases** due to restored electrostatic repulsion. Notably, Na^{+} rejection exceeds K^{+} rejection despite both being monovalent cations—indicating that **hydrated ion size** (Na^{1+}: 0.19 nm; K^{1+}: 0.133 nm; Br^{1-}: 0.196 nm) exerts greater influence on rejection than electrical potential when charge screening occurs.

Increasing TMP enhances convective forcing, promoting ion permeation and **reducing rejection**. Crucially, the **pressure-induced convection potential** outweighs the concentration gradient (diffusion) and residual electrical potential. Therefore, accurate modeling of rejection requires simultaneous consideration of three coupled gradients:

1. **Concentration gradient** (chemical potential),
2. **Electrical potential gradient** (charge interactions),
3. **Applied pressure gradient** (hydrodynamic forcing).

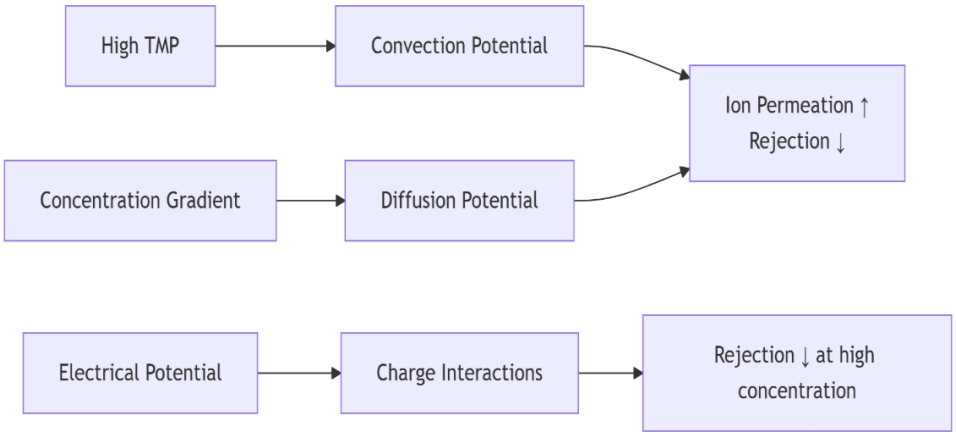

Figure 12. Driving force and ions rejection behavior

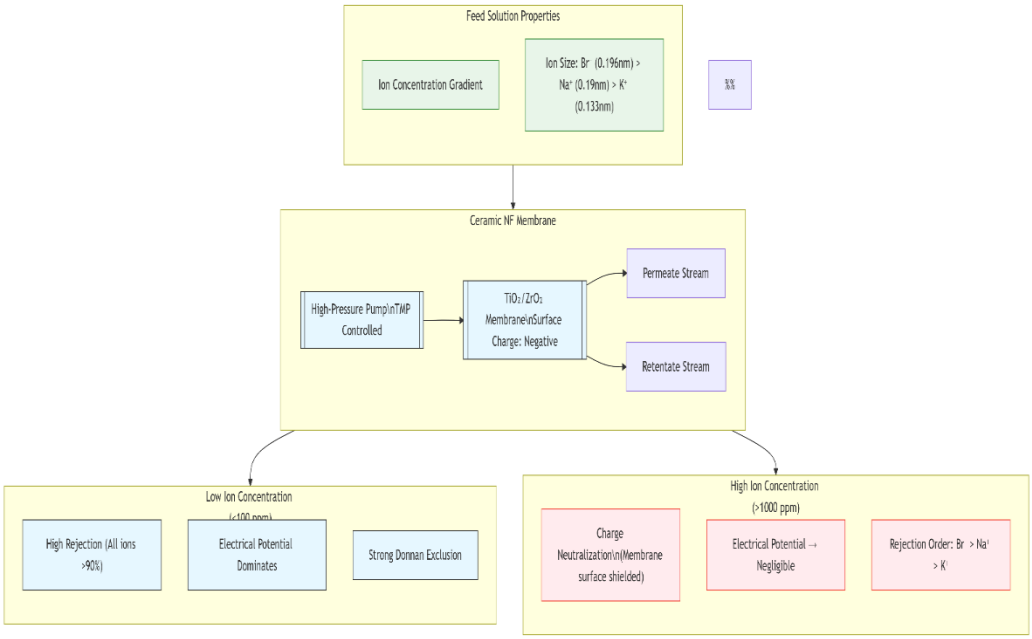

Figure 13. NF membrane separation mechanisms.

Conclusions:

Using a ceramic NF membrane, this research investigated into the separation features of different ions including Mg^{2+}, K^{1+}, Na^{1+}, Br^{1-}, and Cl^{1-} ions using a ceramic NF membrane. Solutions containing double and triple ions were formulated to analyse the separation behaviour of these ions under variable conditions, including trans-membrane pressure and solution concentrations. Specifically, the concentration levels are 0.01, 0.1, 0.5, and 1.0 M and trans-membrane pressure ranges between 1 to 5 bar. The main results indicated that an increase in the trans-membrane pressure generally led to a higher rejection of most ions, except for NaBr and KBr solutions where rejection decreased with increasing trans-membrane pressure. Also, the rejection of most ions decreased with an increase in the solution concentration, except for $MgBr_2$ and KBr mixtures where rejection increased with increasing solution concentration. The research magnificently guaranteed the capability of the ceramic NF membrane to separate various salt mixtures, with variable rejection patterns for individual ions. Statistically, selected ions' rejection varied between 90% to 99.7%. For sodium bromide (NaBr) salt, it was noticed that the rejection of Na^{1+} and Br^{1-} ions decreased as a response to increasing TMP. As the concentration of both Na^{1+} and Br^{1-} ions increased, their rejections increased. However, the maximum rejection

of Br^{1-} ion was at 0.1 M rather than 0.5 M; as in the case of Na^{1+} ion. Implications of research outcomes would be:

A. **Advanced water treatment systems; such as bromide removal and selective ion recovery.** The membrane's exceptional Br^{1-} rejection (peaking at 0.1M) enables targeted removal of carcinogenic brominated disinfection byproducts (DBPs) in drinking water. High Mg^{2+} rejection (90-99.7%) allows magnesium recovery from seawater or industrial wastewater for fertilizer/nutraceutical production.

B. Industrial **process optimization; such as brine concentration and salt fractionation.** Counterintuitive **increased** *r*ejection for $MgBr_2$/KBr at high concentrations (1.0M) supports energy-efficient brine concentration in zero-liquid-discharge (ZLD) systems. An application for **salt fractionation is the** differential rejection of Na^{1+} vs. K^{1+}, which enables separation of NaCl/KCl mixtures for pharmaceutical/food industries.

C. **Membrane technology development, such as pressure management and membrane material science. The** inverse TMP-rejection relationship covers pressure management for NaBr/KBr necessitates pressure optimization protocols (operate at 1-3 bar, not 5 bar). The **material science would be covered by the** ceramic membrane stability at extreme concentrations (1.0M) validates their use in harsh chemical environments where polymeric membranes fail.

Further research can explore the separation of additional salt mixtures, such as $MgBr_2$-$MgCl_2$ and $MgBr_2$-KBr. Also, examining of more complex solutions such as those found in natural water and wastewater would be possible.

Acknowledgement

This project is funded by the scientific research support fund, The Ministry of Higher Education and Scientific Research – Jordan (Eng\1\5\2017).

References

Ahmed, F. E., Ibrahim, Y., & Hilal, N. (2024). Document details - A spacer-based approach for localized Joule heating in membrane distillation. *npj Clean Water, 7*(1). DOI:10.1038/s41545-024-00337-2.

Almandoz, M. C., Pagliero, C. L., Ochoa, N. A., & Marchese, J. (2015). Composite ceramic membranes from natural aluminosilicates for microfiltration applications. *Ceramics International, 41*(4), 5621-5633. DOI: https://doi.org/10.1016/j.ceramint.2014.12.144.

Al-Obaidi, M. A., Kara-Zaïtri, C., & Mujtaba, I. M. (2018). Simulation and optimisation of a two-stage/two-pass reverse osmosis system for improved removal of chlorophenol from wastewater. *Journal of Water Process Engineering, 22*, 131-137. DOI: https://doi.org/10.1016/j.jwpe.2018.01.012.

Al-Obaidi, M. A., Rasn, K. H., Aladwani, S. H., Kadhom, M., & Mujtaba, I. M. (2022). Flexible design and operation of multi-stage reverse osmosis desalination process for producing different grades of water with maintenance and cleaning opportunity. *Chemical engineering researcg and design, 182*, 525-543. DOI: https://doi.org/10.1016/j.cherd.2022.04.028.

Alsarayreh, A. A., Al-Obaidi , M. A., Al-Hroub, A. M., Patel, R., & Mujtaba, I. M. (2020, April 6). Performance evaluation of reverse osmosis brackish water desalination plant with different recycled ratios of retentate. *Computers & Chemical Engineering, 135*. DOI: https://doi.org/10.1016/j.compchemeng.2020.106729.

Ang, W. J., Teow, Y. H., Chang, Z. H., Mohammad, A. W., & Wan, T. W. (2024, September 15). Document details - Innovative ceramic membrane plate filtration system for sustainable semiconductor industry wastewater treatment: A pilot scale study. *Chemical Engineering Journal, 496*. DOI: 10.1016/j.cej.2024.153767.

Arat, S. A. (2023). A review of microplastic removal from water and wastewater by membrane technologies. *Water Sci Technol, 88*(1), 199–219. DOI: https://doi.org/10.2166/wst.2023.186.

Cabrera, S. M., Winnubst, L., Richter, H., Voigt, I., McCutcheon, J., & Nijmeijer, A. (2022, May 17). Performance evaluation of an industrial ceramic nanofiltration unit for wastewater treatment in oil production. *Water Research, 220*, 118593. DOI: https://doi.org/10.1016/j.watres.2022.118593.

Carvalho, A. L., Maugeri, F., Prádanos, P., Silva, V., & Hernández, A. (2011, November 15). Separation of potassium clavulanate and potassium chloride by nanofiltration: Transport and evaluation of membranes. *Separation and Purification Technology, 83*, 23-30. DOI: https://doi.org/10.1016/j.seppur.2011.07.019.

Chen, X., Hong, L., Xu, Y., & Ong, Z. W. (2012, March 20). Ceramic Pore Channels with Inducted Carbon Nanotubes for Removing Oil from Water. *Applied Materials & Interfaces, 4*(4), 1909-1918. DOI:10.1021/am300207b.

Dutta, S., Dave, P., & Nath, K. (2020, February). Performance of low pressure nanofiltration membrane in forward osmosis using magnesium chloride as draw solute. *Journal of Water Process Engineering, 33*. DOI: https://doi.org/10.1016/j.jwpe.2019.101092.

Elfilali, N., Elazhar, F., Dhiba, D., Elmidaoui, A., & Taky, M. (2022, March 4). Performances of various hybrids systems coagulation–ultrafiltration/nanofiltration-reverse osmosis in the treatment of stabilized landfill leachate. *Desalination and Water Treatment, 257*, 55–63. DOI:10.5004/dwt.2022.28360.

Jiang, S., Li, Y., & Ladewig, B. P. (2017, October 1). A review of reverse osmosis membrane fouling and control strategies. *Science of The Total Environment, 595*, 567-583. DOI: https://doi.org/10.1016/j.scitotenv.2017.03.235.

Kim, S. Y., Kim, S., & Park, C. (2025). Evaluation of Ceramic Membrane Filtration for Alternatives to Microplastics in Cosmetic Formulations Using FlowCam Analysis. *Membranes, 15*(35), 1-14. DOI: https://doi.org/10.3390/membranes15010035.

Kirk, C. H., Chong, C. Y., Wang, X., Sun, J., Zhao, Q., & Wang, J. (2024, January 25). Nanofiltration Ceramic Membranes as a Feasible Two-

Pronged Approach toward Desalination and Lithium Recovery. *Global Challenges, 8*(2). DOI: doi.org/10.1002/gch2.202300151.

Kuusik, A., Pachel, K., Kuusik, A., Loigu, E., & Tang, W. Z. (2014, May 15). Reverse osmosis and nanofiltration of biologically treated leachate. *Environmental Technology, 35*(19), 2416-2426. DOI: https://doi.org/10.1080/09593330.2014.908241.

Mdemagh, Y., Hafiane, A., & Ferjani, E. (2018, November 12). Characterization and modeling of the polarization phenomenon to describe salt rejection by nanofiltration. *EDP Sciences, 1*, 1-11. DOI: https://doi.org/10.1051/fopen/2018005.

Mohammad, A. W., Teow, Y. H., Ang, W. L., Chung, Y. T., Oatley-Radcliffe, D. L., & Hilal, N. (2015, January 15). Nanofiltration membranes review: Recent advances and future prospects. *Desalination, 356*, 226-254. DOI: https://doi.org/10.1016/j.desal.2014.10.043.

Mohanadas , D., Nordin, P. M., Rohani, R., Dzulkharnien , N. F., Mohammad, A., Abdul, P., & Abu Bakar, S. (2022, December 29). A Comparison between Various Polymeric Membranes for Oily Wastewater Treatment via Membrane Distillation Process. *Membranes, 1*(46). DOI: https://doi.org/10.3390/membranes13010046 .

Moslemi, M., Davies, S. H., & Masten, S. J. (2012, December). Rejection of Bromide and Bromate Ions by a Ceramic Membrane. *Environmental Engineering Science, 29* (12), 1092–1096.DOI: 10.1089/ees.2012.0086

Schaefer, A., Fane, A. G., & Waite, T. D. (2004). *Nanofiltration principles and applications* (1st Edition ed.). Elsevier Ltd.

Shannon, R. D. (1976). *Acta Crystallographica Section A,Crystal Physics, Diffraction, Theoretical and General Crystallography* (Vol. 32). DOI: https://doi.org/10.1107/S0567739476001551 .

Shocron, A. N., Guyes, E. N., Rijnaar, H. H., Biesheuvel, P. M., Suss, M. E., & Dykstra, J. E. (2021, October 5). Electrochemical removal of amphoteric ions. *The National Academy of Sciences of the United States of America. 118*, pp. 1-12. National Academy of Sciences. Retrieved from https://www.jstor.org/stable/27075934.

Tekoğul, H. (2023, March). Wastewater Treatment of Solid Waste Leachate and Production of Proteinaceous Biomass Using Duckweed Vegetation (Lemna minor). *Journal of Coastal Research, 39*(2), 296-302. Retrieved from https://www.jstor.org/stable/48718190.

Yadav, D., Karki, S., & Ingole, P. G. (2022, August). Nanofiltration (NF) Membrane Processing in the Food Industry. *Food Engineering Reviews, 14*(4), 79 - 595. DOI: 10.1007/s12393-022-09320-4.

Zhang, T., He, Z.-h., Wang, K.-p., Wang, X.-m., Xie, Y.-f. F., & Hou, L. (2022, October 15). Loose nanofiltration membranes for selective rejection of natural organic matter and mineral salts in drinking water treatment. *Journal of Membrane Science, 662*. DOI: https://doi.org/10.1016/j.memsci.2022.120970 .